



HAL
open science

Perspectives for electrochemical capacitors and related devices

Patrice Simon, Yury Gogotsi

► **To cite this version:**

Patrice Simon, Yury Gogotsi. Perspectives for electrochemical capacitors and related devices. *Nature Materials*, 2020, 19 (11), pp.1151-1163. 10.1038/s41563-020-0747-z . hal-03054220

HAL Id: hal-03054220

<https://hal.science/hal-03054220v1>

Submitted on 11 Dec 2020

HAL is a multi-disciplinary open access archive for the deposit and dissemination of scientific research documents, whether they are published or not. The documents may come from teaching and research institutions in France or abroad, or from public or private research centers.

L'archive ouverte pluridisciplinaire **HAL**, est destinée au dépôt et à la diffusion de documents scientifiques de niveau recherche, publiés ou non, émanant des établissements d'enseignement et de recherche français ou étrangers, des laboratoires publics ou privés.



Open Archive Toulouse Archive Ouverte

OATAO is an open access repository that collects the work of Toulouse researchers and makes it freely available over the web where possible

This is an author's version published in:

<http://oatao.univ-toulouse.fr/27014>

Official URL

DOI : <https://doi.org/10.1038/s41563-020-0747-z>

To cite this version: Simon, Patrice and Gogotsi, Yury
Perspectives for electrochemical capacitors and related devices.
(2020) Nature Materials, 19 (11). 1151-1163. ISSN 1476-1122

Any correspondence concerning this service should be sent
to the repository administrator: tech-oatao@listes-diff.inp-toulouse.fr

Perspectives for electrochemical capacitors and related devices

Patrice Simon ^{1,2,3}  and Yury Gogotsi ^{4,5} 

Electrochemical capacitors can store electrical energy harvested from intermittent sources and deliver energy quickly, but their energy density must be increased if they are to efficiently power flexible and wearable electronics, as well as larger equipment. This Review summarizes progress in the field of materials for electrochemical capacitors over the past decade as well as outlines key perspectives for future research. We describe electrical double-layer capacitors based on high-surface-area carbons, pseudocapacitive materials such as oxides and the two-dimensional inorganic compounds known as MXenes, and emerging microdevices for the Internet of Things. We show that new nanostructured electrode materials and matching electrolytes are required to maximize the amount of energy and speed of delivery, and different manufacturing methods will be needed to meet the requirements of the future generation of electronic devices. Scientifically justified metrics for testing, comparison and optimization of various kinds of electrochemical capacitors are provided and explained.

Efficient energy-storage systems are required to power hybrid/electric vehicles and the ever-increasing number of electronic gadgets, as well as storing energy from intermittent sources such as wind and sun. High-performance energy-storage systems are needed in our day-to-day lives in a connected environment, since we all want our electronic devices, such as smartphones and tablets, to hold their charge and operate throughout the day. Electrochemical capacitors (ECs) play an increasing role in satisfying the demand for high-rate harvesting, storage and delivery of electrical energy, as we predicted in a review a decade ago¹. Since then, the need for versatile, ubiquitous, high-power, high-energy-density storage has only increased.

The Ragone plot presented in Fig. 1 demonstrates the status of power versus energy performance of several energy-storage systems available so far. Batteries lie in the high-energy and low-power region, defining a time constant (operation time) ranging from one to tens of hours^{2,3}. They can deliver low power for long stretches and are used in applications ranging from power electronics to mobility and grid storage. The power and lifetime limitations of batteries are caused by the charge-storage mechanism, which involves transformation of chemical bonds via electrochemical redox reactions in the bulk of active materials. The high energy density of Li-ion batteries (up to ~ 300 Wh kg⁻¹) explains why they dominate the market, and this technology is likely to prevail for a long time³. However, battery cycle life is limited to a few thousand cycles, owing to volume changes in the materials upon cycling⁴. Lithium-ion batteries also suffer from a slower recharge rate compared with discharge, owing to Li-metal plating at the negative electrode. Although efforts are ongoing to increase the lifetime and decrease the charging time of batteries, there are fundamental limitations related to solid-state diffusion rate, phase transformations and volume changes on charge/discharge. Also, the energy density of batteries quickly decreases with size, limiting the use of micro-batteries for powering microscale and wearable devices.

ECs are another major family of energy-storage system with electrical performance complementary to that of batteries^{1,5–12}. They can

harvest higher power than batteries but contain lower energy density, resulting in an operation time of tens of seconds to minutes. ECs store the charge via fast, surface-confined processes, which can be electrostatic or faradic in nature^{5,7,10,12}. Such surface storage causes only minor, if any, volume change of the electrode during operation resulting in a long cycle life ($> 10^6$ charge–discharge cycles), as well as a fast charge rate, similar to discharge¹. These key features, together with their energy and power densities, make them useful in applications ranging from small devices for power electronics (power buffer, memory-saving alternating current filtering¹³) to large-size cells and modules for automotive transportation^{14–17}. In the latter, they are used for power delivery but also for energy harvesting, such as braking energy in cars and trams (recharging the EC device via a starter-alternator during vehicle braking steps), which requires high power for a short time (a few seconds). Such applications cannot be achieved with conventional batteries because of the limited power density as well as the charging rate. ECs are also used for grid energy storage for power quality and smoothing, power saving units and frequency regulation, for which the final device weight can reach several tonnes. Supercapacitors are also massively implemented in the electrical pitch control system of wind turbines. In summary, ECs are often used in complement to batteries for short-time (up to tens of seconds) energy delivery and harvesting, that is, when batteries fall short in delivering or receiving power^{15–17}.

Ragone plots (Fig. 1) are widely used in the literature to provide information on power versus energy density of devices, as well as providing a benchmark for various technologies. The coloured areas in Fig. 1 correspond to performance obtained using the same charge and discharge current, whereas areas enclosed by dashed lines refer only to discharge performance (with a recharge at low rate); this presentation highlights the power capability of ECs compared with batteries. Readers must bear in mind that such a plot gives only part of the information. More specifically, although Li-ion batteries can be discharged in a few tens of seconds, the energy efficiency and cycle life will be greatly affected, making ECs preferred for high-rate applications when a long cycle life is required. Caution must be exercised

¹Materials Science Department—CIRIMAT, Université Paul Sabatier, Toulouse, France. ²Réseau sur le Stockage Electrochimique de l'Énergie (RS2E), FR CNRS, Toulouse, France. ³Institut Universitaire de France, Paris, France. ⁴A. J. Drexel Nanomaterials Institute, Drexel University, Philadelphia, PA, USA.

⁵Department of Materials Science and Engineering, Drexel University, Philadelphia, PA, USA. ✉e-mail: simon@chimie.ups-tlse.fr; gogotsi@drexel.edu

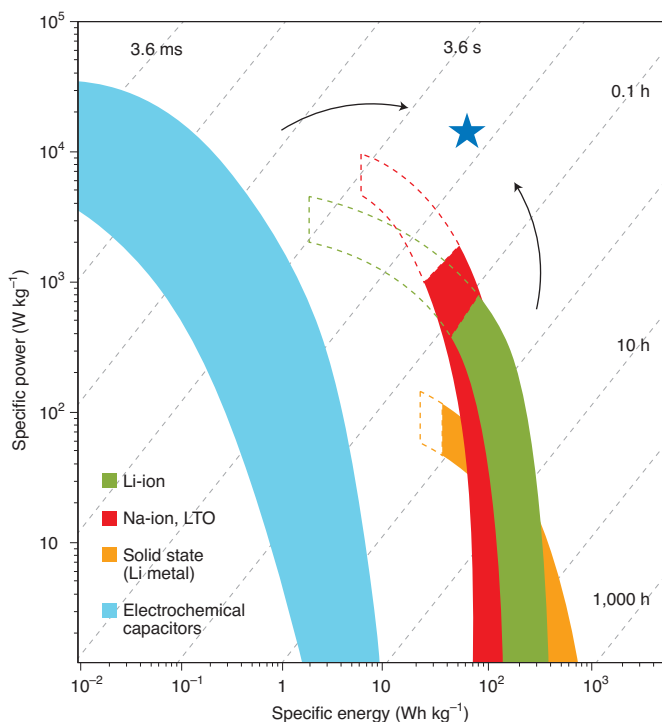


Fig. 1 | Ragone plot. The plot shows the trends towards greater specific power for batteries and specific energy for electrochemical capacitors (arrows), blurring the boundaries between the two as the trends approach the star. Dashed lines represent zones where the cyclability of the device is altered in the case of symmetric cycling (same charging and discharging rate at 100% depth of discharge). For Li-ion batteries, Li plating at the negative electrode is mainly responsible for the decrease in cycle life and the limitation of charging rate. All the data for generating Fig. 1 come from commercial devices (datasheets or real tests). The data for solid state batteries come from industry roadmaps. The diagonal dotted lines and timescales represent characteristic operation timescales, obtained by dividing the energy by the power. LTO, lithium titanium oxide ($\text{Li}_4\text{Ti}_5\text{O}_{12}$).

when reporting performance metrics in Ragone plots, to avoid delivering biased results^{18,19}. Energy and power densities of commercial devices are normalized by the weight (gravimetric) or the volume of the cells (volumetric), which can be easily obtained from direct measurement of cell weight or by cell volume calculation. Materials prepared in the laboratory scale may not be assembled in a realistic cell (with minimized contributions from the electrochemically inactive materials such as electrolyte, current collectors or packaging), so that reporting performance metrics normalized to the total cell weight or volume makes little sense. Extrapolating materials-based performance to a fully packaged cell may lead to unrealistic numbers that deliver the wrong message to the community^{11,18}. Since the cell stack includes current collectors, separators, active material films and electrolyte, energy and power densities normalized per dried cell stack weight or volume should be used (including everything except electrolyte weight). Benchmarking with other commercial devices can be easily achieved by dismantling cells and reporting the same performance metrics: energy and power performance normalized per stack volume or dried stack weight. Following these simple recommendations makes it possible to report trustworthy research results.

Our dependence on electrical energy has only increased over the past decade, and high expectations placed on batteries and ECs make the need to improve performance more relevant than ever. All the research and development efforts aim at pushing ECs and

batteries performance towards the top right part of Fig. 1, which highlights a trend: the boundary between electrochemical capacitors — more specifically ECs based on redox pseudocapacitive materials — and high-rate batteries is becoming increasingly blurred. In the region marked by the star, the high-energy-density challenge for ECs meets the high-power one for Li-ion batteries. For the scientific communities, there is a foundation of common basic science to share and develop (designing and controlling interfaces, material architectures, creating analytical platforms, using modelling and artificial intelligence, and so on).

The next sections of this Review summarize progress in the field of ECs over the past decade as well as showing key perspectives for future materials research, covering porous carbons, pseudocapacitive materials, and the emerging fields of wearable energy storage and of microdevices and fabric supercapacitors for the Internet of Things (IoT).

Electrical double-layer capacitors

Electrical double-layer capacitors (EDLCs) store charge electrostatically through reversible adsorption of electrolyte ions onto electrochemically stable, high-surface-area carbon materials^{1,20}. Charge separation occurs upon polarization at the electrode/electrolyte interface, producing what Helmholtz described in 1853 as the double-layer capacitance, C (see also Fig. 2)^{1,21}.

$$C = \frac{\epsilon_0 \epsilon_r A}{d} \quad \text{or} \quad \frac{C}{A} = \frac{\epsilon_0 \epsilon_r}{d} \quad (1)$$

where ϵ_r is the electrolyte dielectric constant, ϵ_0 is the dielectric constant of the vacuum, d is the effective thickness of the double layer (charge separation distance) and A is the electrode surface area. The absence of any faradic contribution in the charge-storage mechanisms explains the specific electrochemical signature, from a rectangular box-shaped cyclic voltammogram to a sloping profile during galvanostatic charge discharge (Fig. 2a). Although EDLCs are the main commercialized EC devices, they suffer from limited energy density (equation (2)), and their challenge is to increase the amount of energy stored.

$$W = \left(\frac{1}{2}\right) \frac{CV^2}{3,600}, \quad (2)$$

where C is the capacitance (in farads), V the cell voltage (volts) and W the energy (watt hours).

Although high capacitance ($>200 \text{ F g}^{-1}$) could be achieved by adding redox functions^{1,12} (such as by doping carbon with heteroatoms²²), the limited cell voltage of aqueous electrolytes (typically less than $\sim 1.5 \text{ V}$) due to water electrolysis has so far hampered the development of aqueous technology. Today, commercial EDLC cells use non-aqueous electrolytes — typically $1 \text{ M } (\text{C}_2\text{H}_5)_4\text{N}^+, \text{BF}_4^-$ dissolved in acetonitrile or propylene carbonate — that yield an average cell voltage of 2.7 V (refs. ^{23,24}).

Self-discharge is an important parameter for ECs. It can originate from charge recombination at the surface of the porous carbon electrode by diffusion of ions from the double layer to the electrolyte, or from the presence and consumption of redox impurities such as surface functional groups and/or water traces in the organic electrolyte²⁰. Although the self-discharge of ECs is higher than that of batteries owing to the different charge-storage mechanism (electrostatic or surface redox versus bulk redox), commercial ECs have now reached low leakage current (a few microamps per farad at the maximum voltage at room temperature)¹⁵. Such low values for the leakage current correspond to several weeks to move from the maximum voltage to half voltage once the cell is charged. Additionally, being high-power devices, supercapacitor banks may need a thermal management system to dissipate the heat generated during

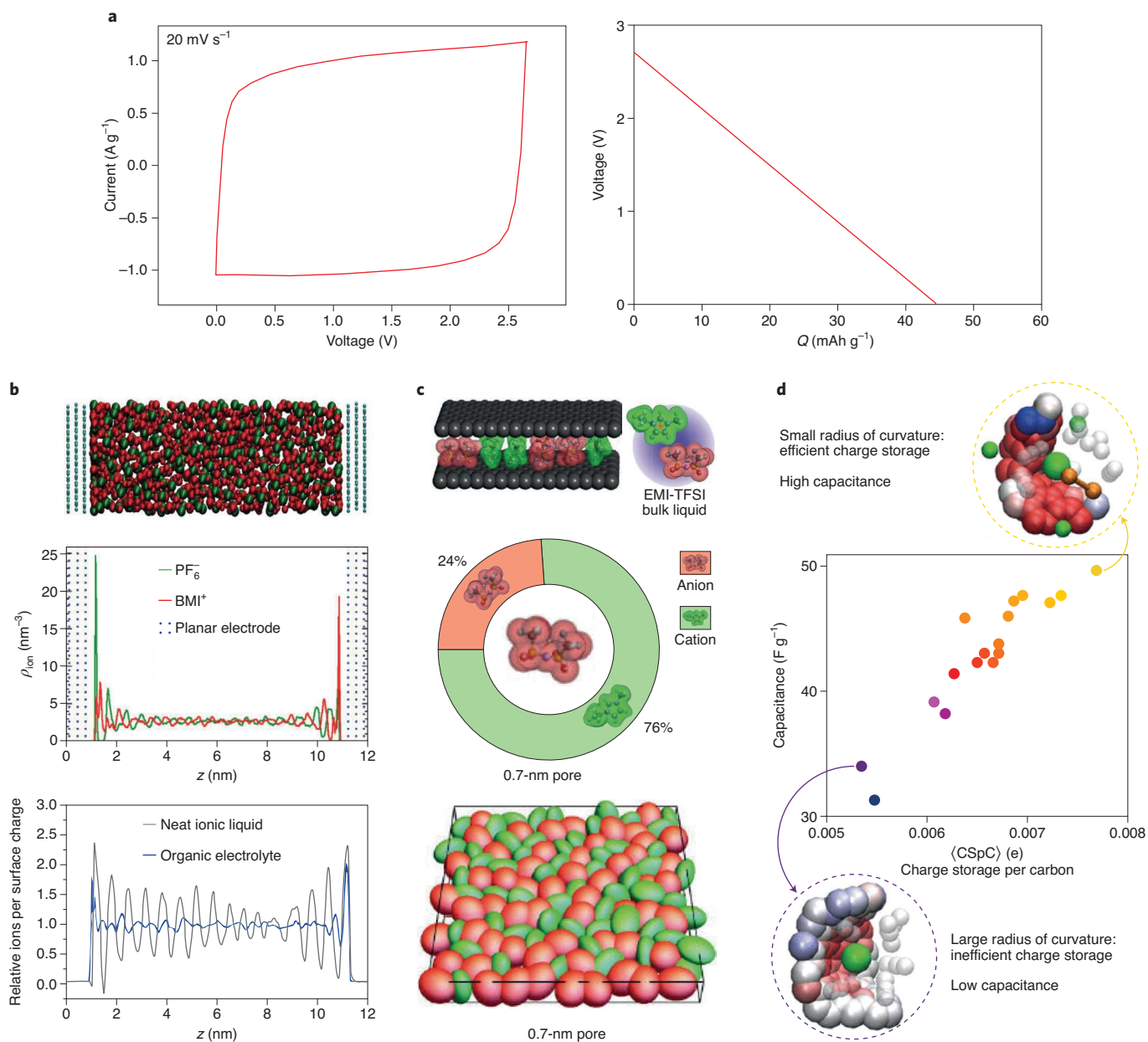


Fig. 2 | Carbon-based electrical double-layer capacitors. **a**, A typical CV (left) and a galvanostatic discharge plot (right) of a capacitive EDLC; Q is the gravimetric capacity normalized to carbon weight. **b-d**, Charge-storage mechanisms. **b**, Snapshot of BMI,PF₆ ionic liquid electrolyte between two graphite electrodes under a polarization of 2 V (top). The long-range layered structure observed as a consequence of charge overscreening (middle) is suppressed when adding an organic solvent (bottom). ρ_{ion} , ion density. **c**, Formation of a superionic state as the consequence of the creation of co-ion pairs when the ionic liquid EMI-TFSI is confined in pores with a size comparable to the ion size (top). The first solvation shell around an anion contains up to 24% anions without polarization (middle). This results in increased ion population in the pores (bottom). **d**, The charge stored per carbon in nanopores of 3D porous carbons increases with the decrease of the curvature radius, as the consequence of stronger/closer interactions of the confined ions with the carbon walls. Adapted with permission from: **c**, ref. ⁵³, SNL; **d**, ref. ⁵⁵, American Chemical Society, with the help of Y. M. Liu. Panel **b** courtesy of Celine Merlet.

operation. However, compared with high-power batteries (using Li₄Ti₅O₁₂ anodes or LiFePO₄ cathodes, for instance), the lower series resistance of ECs decreases the polarization and heat generation^{25,26}.

Key advances have been made during the past decade in understanding the basic science driving the formation and charge of the double layer in nanoporous carbon electrodes^{10,12,27,28}, starting in 2006 with the pivotal discovery of the capacitance increase in subnanometre carbon pores²⁹. In situ characterization tools, such as nuclear magnetic resonance (NMR)^{28,30-32}, neutron and X-ray scattering^{27,33}, mass spectrometry³⁴, Raman and infrared spectroscopies^{35,36},

combined with modelling^{30,37-41}, were adapted to tracking ion fluxes and adsorption in nanopores. Electrochemical quartz-crystal microbalance experiments (not only in conventional gravimetric modes^{31,42} but also in modified dissipation^{43,44} or a.c.-gravimetric modes⁴⁵) and atomic force microscopy experiments^{46,47} revealed the electrolyte dynamics and ion adsorption during operation. These research efforts led to revisiting the basic concept of the Helmholtz double-layer formation at planar^{48,49} and nanoporous carbon electrodes. They also brought about a better understanding of the origin of this capacitance increase. The increase is now attributed to the

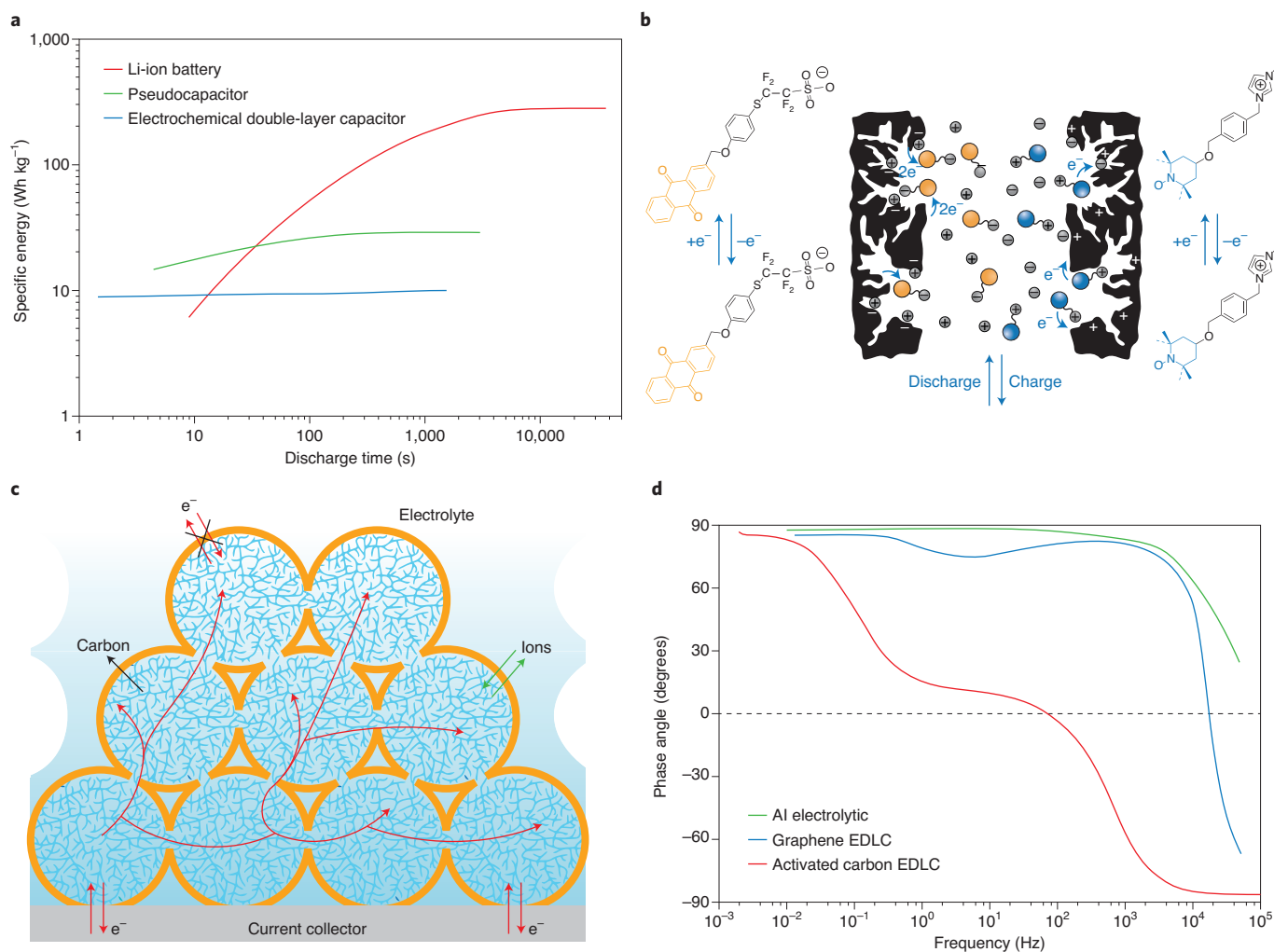


Fig. 3 | Current performance of carbon-based electrical double-layer capacitors and perspectives for improvements. **a**, Comparison of discharge energy at various discharge times for a Li-ion battery (red), a pseudocapacitor (green) and an EDLC (blue) of similar volume. For discharge times less than ~ 10 s, EDLCs can deliver higher energy density, while the discharge time should reach ~ 30 s for the current generation of pseudocapacitors. **b**, Concept of biredox electrolyte, in which anions and cations are functionalized with redox active species to contribute to the charge-storage mechanism in addition to double-layer storage. **c**, Surface modification of porous carbon electrodes (passive layer, for instance) to enlarge the operating voltage window. The passive layer (orange colour) blocks the electron transfer at the electrolyte/carbon interface (double red arrows), and allows for ion transfer (double green arrows). The electrical percolation is ensured by the carbon grains in the volume of the electrode (red arrows) and by direct contact of the carbon electrode with the current collector. **d**, Ultra-high-rate graphene-based EDLC for a.c. to d.c. conversion, which can compete with aluminium electrolytic capacitors for filtering applications. Adapted with permission from: **a**, ref. ⁵⁷, The Electrochemical Society, IOP; **d**, ref. ¹³, AAAS. Panel **b** Credit: O. Fontaine

partial desolvation of ions resulting in ion accessibility to subnanometre pores^{27,28,30,31,39,42,43,50,51}, leading to a specific organization of the electrolyte confined in these nanopores^{51,52} as well as the creation of image charges^{40,53} on the carbon surface, and denser ion packing^{39,54,55}. Figure 2b–d summarizes the current understanding of EDLC theory provided by these theoretical and computational studies. While, as a consequence of the charge overscreening, a relatively long-range layered structure is observed for a neat ionic liquid electrolyte at planar graphite electrodes under polarization, the presence of solvent breaks the electrolyte organization (organic electrolyte; see Fig. 2b). The confinement of a neat ionic liquid electrolyte in pores with a size comparable to the ion size results in the formation of a superionic state with the creation of co-ion pairs, thus improving the capacitance (Fig. 2c). In nanopores of three-dimensional (3D) carbons, the capacitance increase observed for small pore sizes is the result of the absence of overscreening, thus reducing the effective double-layer thickness and causing stronger/closer interactions of ions with carbon walls due to the confinement (Fig. 2d).

These results show that carbons with average pore size below 1 nm can suppress the diffuse layer and take advantage of the overscreening effect. A counter-ion charge-storage mechanism (adsorption of ions of the opposite charge of the carbon) may be preferred, rather than an ion exchange mechanism, to limit ion fluxes and associated decrease of ion transport^{31,42,48}. While NMR studies have shown that the confinement affects the ion dynamics by decreasing the self-diffusion coefficient in pores by two orders of magnitude²⁸, ion transport is still fast enough in these small and short pores to ensure low resistance and high power performance^{1,12,29}. Also, pores possessing ionophobic character have shown faster ion transport in non-aqueous electrolytes compared with ionophilic ones³⁷. In neat ionic liquids, the creation of image charges on the carbon surface resulted in the creation of co-ion pairs in nanopores, also called a superionic state, associated with important capacitance enhancement^{53,56}.

Interestingly, those scientific advances were transferred into real commercial EDLC products in the way that carbon manufacturers modified their synthesis process to prepare activated carbons

with an average pore size in the nanometre range¹⁷. As a result, the energy density of current commercial EDLCs (currently up to 10 Wh kg⁻¹)¹⁷ exceeds by a factor of 2 that of devices of the same size in 2005 (<4 Wh kg⁻¹), and current EDLCs can deliver high power for tens of seconds, thus nicely replacing or complementing batteries in a number of applications⁵⁷ (Fig. 3a). However, the whole picture of the ion transport and adsorption in carbon nanopores is not yet clear, and fundamental studies are still needed to better understand the ionic fluxes inside large nanoporous networks with a variety of pore shapes, connections between pores, and pore-wall structure and properties.

Although important, fine-tuning the porous carbon structure to take advantage of the electrolyte confinement effect may not be able to bring the energy density beyond 20 Wh kg⁻¹, as required for a major expansion of the market for EDLC devices. A way to increase the carbon capacitance is to graft electroactive molecules on porous carbon electrodes, thus adding a redox contribution to the double-layer capacitance. In such an approach, pioneered by Bélanger and co-workers, grafting anthraquinone^{58,59} from diazonium salts led to a considerable increase in capacitance in aqueous electrolytes. However, stability remains a concern, as part of the redox molecules is adsorbed on the carbon and not grafted, and their further release into the electrolyte may lead to capacitance decrease with time and reduced cycle life.

Alternatively, increasing the cell voltage would be even more rewarding as regards energy improvement (see equation (2)). Cell voltage is driven by the electrochemical stability window of the electrolyte and the presence of electrochemically active surface functional groups at the porous carbon surface. Commercial cells rated at 3 V have recently been developed by careful removal of oxygen-containing terminations from the porous carbon surface^{15,16}. Interestingly, model materials such as graphene or carbon nanotubes with surfaces free from any functional groups have shown substantial improvement in cell voltage. Recent work from Kyotani and co-workers, using mesoporous carbon sheets prepared by chemical vapour deposition from CH₄ on nanosized sacrificial templates made of alumina particles, demonstrated cell voltages up to 4.4 V (ref. 60). The prepared mesoporous structure with curved graphene walls was free from reactive edge-sites and demonstrated a large voltage window. These studies with model materials provide the scientific foundations for the design of ultra-stable porous carbon structures with improved performance. On the other hand, Antonietti's group reported heteroatom-doped carbons known as 'noble carbons', obtained by carbonization of organic compounds⁶¹. These carbons show improved electrochemical stability versus oxidation, and could lead to substantial energy gain, as long as their electrical conductivity remains high enough for them to be used as active material.

The design of a high-voltage electrolyte (>5 V stability window) matching the requirements for energy-storage applications (high conductivity, large operation temperature range, low toxicity) is a major challenge for battery and EC communities, and there is still no certainty that it will become industrial reality. However, interesting approaches to tailoring electrolytes for EC applications have recently been proposed²³. For instance, Balducci and co-workers proposed a combinatorial chemistry approach to select new solvent/salt couples by rational computational screening^{62,63}. This identified the cyano-esters family as a new class of possible solvent, and especially the 3-cyanopropionic acid methyl ester. In combination with the conventional (C₂H₅)₄N⁺,BF₄⁻ salt, a cell operating voltage up to 3.2 V was achieved, which confirms the potential of the method and justifies further use of machine learning and artificial intelligence, owing to the large variety of combinations possible²³. A new concept, proposed by Rochefort and co-workers⁶⁴ and by Fontaine and co-workers⁶⁵, has emerged, in which the charge storage could also be achieved in the electrolyte (Fig. 3b). It relies on the use of redox ionic liquids as salt in an electrolyte to achieve bulk-like

redox density with liquid-like fast kinetics. The cation and anion of these redox ionic liquids bear moieties that undergo very fast, reversible redox reactions, increasing the charge storage by transferring electrons at the negative (reduction) and positive (oxidation) electrodes^{64,65}. The capacitance of the porous carbon electrode was found to be twice as large for 0.5 M redox salts in BMIm-TFSI (1-butyl-3-methylimidazolium bis(trifluoromethylsulfonyl)imide) electrolyte compared with redox-free solution⁶⁵. The concept sounds appealing, and more work will be needed to (i) understand the charge transfer mechanism including possible self-discharge processes and (ii) synthesize redox moieties with high capacity and tuned electrode potentials to further improve the performance. Increased voltage window and carbon capacitance was also recently reported by using solvent-free ionic liquid electrolytes^{51,52}, involving ion reorganization inside the micro/mesoporous carbon network. These processes rely on local anion-cation exchange processes on the angstrom scale, resulting in short time response.

Alternatively, cell voltage improvement could be obtained by modifying the electrode/electrolyte interface via the design of passive layers at the carbon surface, which would shift the electrolyte reduction and/or oxidation reactions to higher over-voltages (Fig. 3c). This is basically what is happening at graphite anodes during Li-ion intercalation in Li-ion batteries, where a solid electrolyte interphase (SEI) spontaneously forms on the graphite particle surface⁶⁶. Once formed during the first cycle, the SEI layer prevents further electrolyte reduction while allowing Li-ion intercalation into the graphite underneath. In a similar way, designing specific, tailored properties of the carbon surface (hydrophobic or hydrophilic groups, for instance) could yield an important over-voltage to increase the electrochemical stability window of the electrolyte. Those approaches based on modification of the carbon/electrolyte interface are certainly appealing in terms of opportunities for performance improvement but are highly challenging. The surface modification must not alter or hinder the access of the ions in the electrolyte to the porous carbon structure. The modified carbon surface must be ionically conductive to allow ion transfer from the electrolyte into the carbon pores but electrically insulating to limit solvent oxidation and/or reduction at the carbon surface. The concept of the passive layer was recently applied to Li-metal⁶⁷ and Mg-metal⁶⁸ anodes for Li-metal and Mg-metal batteries, respectively. The successful design of such an artificial SEI-like layer (rather than the one formed spontaneously for graphite anodes) on the surface of porous carbon would greatly boost the EDLC performance. Mastering the electrode/electrolyte interface is also a key challenge for Li-ion batteries; this is particularly true with the current trend to develop all solid-state Li-ion batteries based on inorganic ceramic electrolytes. There is then a common interest in developing and sharing techniques for characterizing the electrode/electrolyte interface, as well as underlying basic science^{12,27,31,32,34,52}.

In addition to increasing the voltage window, capacitance and energy density, substantial expansion of the temperature window has been achieved by using non-freezing mixed electrolytes (for example, eutectic mixtures of ionic liquids or mixed solvents) and minimizing diffusional limitations via carbon material design. As a result, ECs operating at temperatures down to -75 °C for space applications⁶⁹ or across the -50 °C to 100 °C range have been reported^{70,71}.

There is another growing trend in using high-power EDLCs to challenge the conventional aluminium electrolytic capacitors in energy harvesting, back-up and even alternating-current (a.c.) filtering applications^{7,13,72}. Whereas conventional porous-carbon-based (activated carbon) EDLCs become resistive at frequencies above 1 Hz, non-porous carbons such as carbon black⁷² or vertically grown graphene⁷³ can operate at much higher frequencies (Fig. 3d). As the capacitance of aluminium electrolytic capacitors is limited to microfarads or millifarads, replacing them with EDLCs with a

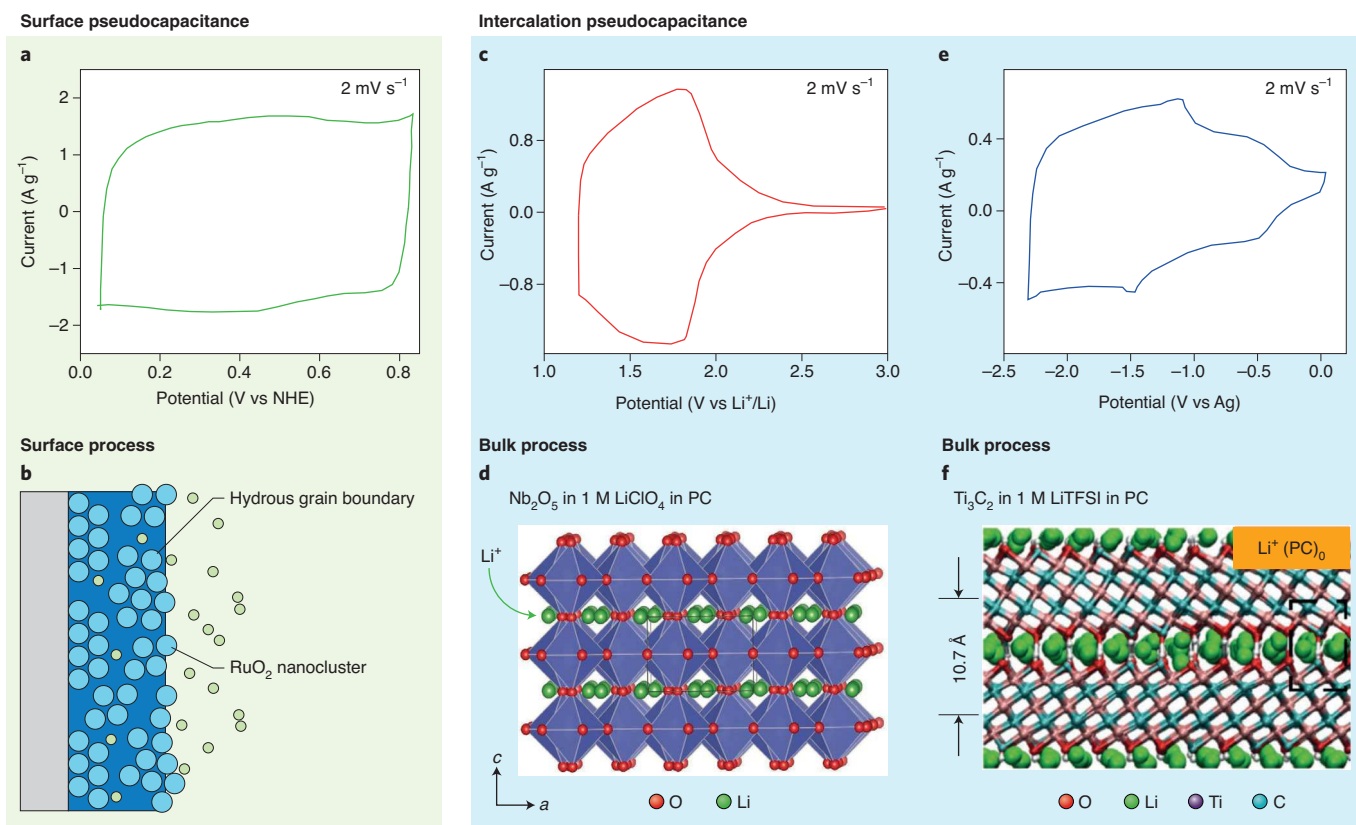


Fig. 4 | Conceptual presentation of redox capacitance. **a**, CV of RuO₂ electrode. **b**, The fast surface reactions at RuO₂ particles explain the presence of bumps on a capacitive-type CV, leading to a surface pseudocapacitance charge-storage mechanism. **c**, Electrochemical signature (CV) of T-Nb₂O₅ in non-aqueous LiClO₄ in propylene carbonate (PC) electrolyte, showing intercalation pseudocapacitance due to fast, non-diffusion-limited Li⁺ intercalation into the bulk of the material. **d**, Structure of T-Nb₂O₅ with the intercalated Li ions. **e**, CV of a Ti₃C₂ MXene electrode in non-aqueous 1 M LiTFSI in PC electrolyte, showing fast Li⁺ intercalation into the gaps between Ti₃C₂ layers. **f**, Structure of Ti₃C₂ MXene showing intercalated and desolvated Li ions (noted as Li⁺(PC)_n) between the Ti₃C₂ MXene layers. Adapted with permission from: **a,b**, ref. ¹², SNL; **e,f**, ref. ⁸⁶, SNL.

capacitance orders of magnitude higher is attractive. Higher volumetric capacitance, extreme cyclability (over a million cycles at a very high rate) and scalable device manufacturing must still be achieved, and the phase angle should be closer to 90° across a wider range of frequencies. Large-scale flexible supercapacitors that can provide both high volumetric and high areal capacitance, as well as a high-frequency (>100 Hz) capacitive response with a phase angle approaching -90°, are expected to resolve the current impediment for high-power applications.

In summary, EDLCs are a class of ECs that store the charge electrostatically without involving any redox reactions, providing high delivery/uptake power capability and ultra-long life (>10⁶ cycles). These key features make them suitable in a broad range of applications including renewable energy and grid storage (power smoothing, phase regulation, uninterruptible power supplies), as well as transportation (stop and start function, recovery of braking energy, power steering), where they offer specific added value compared with batteries. Although electrolyte confinement in carbon nanopores came with substantial improvement in their capacitance and energy density, alternative routes must be found to further improve the performance. Efforts should be directed towards the design of high-surface-area carbon structures with improved electrochemical stability. Also, modification of the porous carbon/electrolyte interface by preparing passive layers or designing specific properties (hydrophobicity or hydrophilicity) may offer more opportunities to enlarge the operation voltage range of EDLC devices — but this must be achieved without sacrificing power capability or cycle life.

Pseudocapacitive and high-charge/discharge-rate materials based on redox capacitance

Unlike in EDLCs, the charge-storage mechanism in pseudocapacitive materials is not purely electrostatic. It involves faradic processes — redox reactions^{1,5,20,74} that increase the capacitance and thus the energy density of supercapacitors (Fig. 3a). The surface redox pseudocapacitive mechanism was proposed in the 1970s by Conway, who explained that when reversible redox reactions occur at or near the surface of an appropriate electrode material, the electrochemical features are those of an EDLC but with considerably greater charge storage because of the redox reactions²⁰. Materials such as MnO₂ and RuO₂ (Fig. 4a) were among the first reported examples of pseudocapacitive materials^{20,75}. In these materials, the change in the redox state of the metal is balanced by the surface insertion/deinsertion of a cation from the electrolyte. The redox reactions are confined to the surface — or the near-surface volume — of the material, differentiating it from the bulk faradic storage in battery materials^{20,74,76,77}. This results in a rectangular-shaped cyclic voltammetry (CV) curve (Fig. 4a), similar to that of EDLCs.

Different from faradic reactions occurring in the bulk of (battery) materials, the pseudocapacitive mechanism (or redox capacitive mechanism) has the following characteristic features: (i) a charge that changes with the potential; (ii) the absence of solid-state diffusion limitation, owing to the surface or near-surface storage mechanism (surface pseudocapacitance; see Fig. 4b); and (iii) the absence of phase change in the material during electrochemical polarization, which would result in sharp redox peaks in the CVs^{3,74,76–78}.

These criteria result in symmetrical CV curves along the potential axis, where the peaks, if present, are broad and exhibit a small peak-to-peak voltage separation.

The faradic nature of the charge-storage mechanism makes the use of charge or capacity (in coulombs or amp hours) a suitable metric to characterize pseudocapacitive materials. Although capacitance (in farads) may be given for comparison purposes, it is meaningless to report capacitance values from distinctly non-rectangular-shaped CVs. Electrochemical impedance spectroscopy plots in the Nyquist representation shows a sharp, almost vertical, increase of the imaginary part of the impedance in the low-frequency region as the result of the absence of solid-state diffusion^{5,76–78}. Several electrochemical methods and techniques have been developed to help in the characterization of pseudocapacitive materials, such as the identification of the surface versus bulk contributions to the total current⁷⁹, as well as the use of electrochemical impedance spectroscopy at various potentials⁸⁰ or multiple step potential techniques^{81,82}. These tools must be used by the scientific community to correctly characterize materials and report their performance, avoiding misleading reports, such as capacitance values exceeding $1,000 \text{ F g}^{-1}$ for faradic nickel oxide or oxy-hydroxide in alkaline electrolyte^{5,19,76–78}. Interestingly, using cobalt oxide as a model material, a recent report explains its pseudocapacitive electrochemical signature (similar to Fig. 4a and to the one observed for MnO_2 in neutral electrolyte) by a transition from an insulating to an electrically conducting phase initiated by redox reaction⁸³. In this material, the creation of a potential gradient would result in a double-layer capacitance-like storage mechanism, but more experimental work (using in operando structural analysis, for instance) is required to support such a claim.

Although pseudocapacitive materials hold promise for improving the energy density of EC, they have so far not seen widespread use in commercial products because of (i) the high costs of RuO_2 , (ii) the limited capacitance and low electrical conductivity of MnO_2 and other metal oxides, (iii) the short lifetime of conducting polymers and (iv) the restriction of the pseudocapacitive behaviour to aqueous electrolytes with a narrow voltage window. However, the discoveries and advances of the past few years on metal oxides and carbides could change the game. In 2011, a family of 2D early transition metal carbides and carbonitrides (MXenes) was produced by selective etching of the A element from MAX phases⁸⁴. MXenes are usually referred to as $\text{M}_{n+1}\text{X}_n\text{T}_x$, where M is an early transition metal and X is carbon and/or nitrogen, T represents surface termination ($=\text{O}$, $-\text{OH}$, $-\text{Cl}$ and/or $-\text{F}$), $n = 1, 2, 3$ or 4 , and x is the number of terminating groups per formula unit⁸⁵. $\text{Ti}_3\text{C}_2\text{T}_x$ MXene has been intensively studied for energy-storage applications^{85,86}. CV of this material in sulfuric acid electrolyte shows broadened peaks with little separation in peak position on charge/discharge, on top of a capacitive rectangular box (Fig. 4a). In this material, the change of the valence state of the surface layers of Ti atoms ($\text{Ti}^{\text{II}}/\text{Ti}^{\text{III}}$) is balanced by the reversible intercalation reaction of protons⁸⁵. Needless to say, the metal-like conductivity of $\text{Ti}_3\text{C}_2\text{T}_x$ MXene excludes the possibility of a pure double-layer-like mechanism coming from the change in the electrical conductivity during polarization⁸³. High gravimetric capacitance ($>500 \text{ F g}^{-1}$)^{85,87} and volumetric capacitance ($1,500 \text{ F cm}^{-3}$), with an areal capacitance of up to 4 F cm^{-2} (ref. ⁸⁸), were obtained in aqueous sulfuric acid electrolyte. Moreover, 50% of the capacitance could be delivered (or stored) during 1 s discharge (charge). These impressive performance is the result of the combination of 2D structure that offers redox-active surface highly accessible to electrolyte ions, and short transport paths, together with the high electrical conductivity of the MXene backbone, which makes these materials unique⁸⁵. As MXene electrodes usually do not require the use of metallic current collectors (at least in prismatic and pouch cells), the energy density of the devices can be given an extra boost^{85,89}.

Still, according to the results outlined above, the narrow voltage window (typically about 1 V) limits the energy density (equation (2)) for pseudocapacitive materials operating in aqueous electrolytes; this is an important drawback that hampers the industrial application of the technology. Possible remedies include the use of water-in-salt electrolytes with a wider voltage window (2 V or more), as well as asymmetric device design with, for example, a MXene negative electrode combined with an oxide or conducting polymer cathode, extending the voltage window above 1.5 V. Both approaches can be combined for maximum performance improvement.

In 2013, Dunn's group reported on the synthesis of nanocrystalline orthorhombic-phase Nb_2O_5 particles ($\text{T-Nb}_2\text{O}_5$)⁹⁰, with controlled structure and texture, capable of working in a non-aqueous electrolyte. The Li-ion intercalation capacity was mostly independent of rate, and redox peaks with small voltage offsets were observed even at high rates. Moreover, the Li ion intercalation reaction was found to occur in the bulk of the particles, thanks to facile 2D lithium-ion diffusion pathways existing in the orthorhombic crystal structure^{74,90,91}. Together with the absence of any phase transformation, these agreed well with a Li-ion intercalation pseudocapacitive reaction mechanism⁷⁴ such as defined by Conway⁹² (Fig. 4c), which needs a network that offers 2D transport pathways and little structural change on intercalation. Mirror-like CVs in non-aqueous electrolytes, with broad redox peaks on top of a capacitive envelope, are characteristics of such materials. Here, the change of redox state of Nb during Li ion intercalation, together with high capacity (150 mAh g^{-1}) values achieved, also excludes the possibility of a pure double-layer mechanism contribution. Interestingly, this material combines the key features of faradic (battery) and pseudocapacitive materials, namely (i) high capacity thanks to Li ion intercalation into the bulk of the particles and (ii) high power because of the high rate, non-diffusion-limited reaction in the facile 2D Li-ion diffusion pathways of the structure (Fig. 4d).

The intercalation pseudocapacitive behaviour of Ti_3C_2 MXene electrodes in Li-ion-containing non-aqueous electrolyte has recently been reported in the literature (Fig. 4e)⁸⁶. Capacity up to 130 mAh g^{-1} was achieved in 1M Li-TFSI in propylene carbonate (PC) electrolyte, within a 2.4-V voltage window (from $\sim 2.8 \text{ V}$ down to 0.4 V versus Li). The high capacitance in PC-based electrolytes was ascribed to the full desolvation of Li ions when intercalated between the MXene layers, resulting in improved Li ion intercalation compared with other solvents⁸⁶. Similar to Nb_2O_5 , the intercalation is not limited by solid-state diffusion in MXene, thanks to the combination of the 2D structure offering 2D paths for Li ion intercalation and the metallic conductivity of Ti_3C_2 which results in high power performance. Interestingly, Li-ion desolvation was found to be responsible for the high performance of MXene in non-aqueous electrolyte (Fig. 4f), similar to what was reported earlier for porous carbon^{1,29}. Finally, in very recent work⁹³, F-free MXene materials prepared by a molten salt synthesis route achieved unique electrochemical performance in terms of energy and power density in Li-ion battery electrolyte. The control of the surface termination groups and Li-ion desolvation allowed the use of this MXene as high-rate negative electrode material for electrochemical energy storage, with capacities reaching 200 mAh g^{-1} .

There are currently few commercial devices operating with pseudocapacitive materials. These materials still have a limited cycle life and power performance compared with EDLCs, without offering a cost advantage. Although the recently developed MXene materials appear promising for high rate pseudocapacitive electrodes, improvements are needed in the irreversible capacity loss due to SEI formation, the control of the nature and content of surface termination groups, and the synthesis routes. However, research over the past few years has resulted in great advances in both the basic science and practical performance. Further efforts will be needed

to move pseudocapacitive oxides, carbides, nitrides and other materials to the market.

Beyond offering promising power and energy performance, these examples illustrate changes of paradigm in the design of redox-based capacitive materials for high-energy ECs. The frontier between high-discharge-rate battery materials and pseudocapacitive materials, which combine the best of the battery and EDLC worlds, becomes increasingly blurred^{10,12}. Moreover, it is possible to transform the electrochemical signature of a faradic battery material into a pseudocapacitive one by decreasing the particle size and/or introducing defects in the structure, as has been achieved with LiFePO₄ (refs. ^{94,95}) LiCoO₂ (ref. ⁹⁶) and other cathode materials⁷⁴. These materials are called extrinsic pseudocapacitive materials^{5,74} to distinguish them from conventional intrinsic pseudocapacitive materials (Fig. 4). In these materials, high defect concentrations (breaking the crystal structure) and large surface area, which can be achieved by adapting the synthesis route or nanosizing the particles, accelerate the Li solid-state diffusion^{74,95,96}. A striking example is LiFePO₄ (LFP), a well-known positive electrode material for Li-ion batteries. Li-ion intercalation into LFP is achieved via a two-phase reaction mechanism, resulting in a constant potential plateau at 3.5 V versus Li during constant-current charge/discharge tests. The modification of the LFP structure with Fe³⁺ defects, for instance⁹⁵, yields a different electrochemical behaviour. Constant-current charge/discharge tests of amorphous LFP containing Fe³⁺ defects show sloping potential profile change with time, like observed for intercalation pseudocapacitance mechanism. The change in electrochemical behaviour of the defective LFP was ascribed to faster Li-ion diffusion in the presence of defects^{94,95}. The past few years have seen a growing number of papers dealing with the synthesis and characterization of high-rate materials with pseudocapacitive or pseudocapacitive-like signature for both negative and positive electrodes^{7,10,97}. This looks like a promising way to improve the energy density of ECs and exceed the power density of batteries.

In summary, pseudocapacitive materials have the potential to improve the energy density of ECs considerably. However, conventional pseudocapacitive materials (such as RuO₂, MnO₂ or Fe₃O₄) are only active in aqueous electrolytes, limiting their energy density and practical applications. The past decade has seen rapid development of research on these materials. Designing 2D materials or metal oxides with crystal structure offering 2D Li-ion diffusion pathways for fast Li intercalation in non-aqueous electrolyte has led to evidence of a fast intercalation mechanism in the bulk of the material ('intercalation pseudocapacitance'). Also, the modification of faradic battery materials by creating defects in the structure and incorporating structural water, as proposed by Augustyn and co-workers^{98,99}, yields pseudocapacitive signatures and offers opportunities for designing high-energy and high-power-density pseudocapacitive ECs.

At the same time, as we have said, the boundary between high-rate battery materials and high-energy pseudocapacitive materials is becoming increasingly blurred. This holds promise for great improvement in the energy density while maintaining a high power capability and a long cycle life (>1,000,000 cycles), moving to the area marked with the star in Fig. 1. Some general guidelines can be given for extending the energy density of high-rate pseudocapacitive materials, most of them being shared with the battery community. First, a negative (positive) electrode must deliver/store its charge at the lowest (highest) average potential, to end up with the highest cell voltage and energy density. Next, the presence of a SEI layer and the risk of Li plating at high recharge rate are important drawbacks when using negative electrodes operating at low potentials in Li-containing electrolyte. This is why new materials based on intercalation capacitance (metal oxides, such as Nb₂O₅, LiTiNb₂O₇ or Li₃VO₄, and MXenes) operating at high rate with no — or limited — risk of Li-metal plating are attractive candidates, despite

their higher discharge potential. As positive electrodes, high-rate, Li-containing materials are also good candidates since they can supply Li ions to the negative electrode, in case SEI is formed at the first cycle. Defective LFP is a possible candidate, but such an approach could be extended to lamellar transition metal oxides operating at higher potentials. Those redox-based capacitive materials could also benefit from the development of solvent-in-salt electrolytes, which can achieve improved operating voltage window in combination with Li-ion battery electrodes, thanks to the decrease of the content of free solvent molecules¹⁰⁰.

Hybrid capacitor design

There is plenty of basic science to share and develop between the battery and the capacitive storage communities, and a common playground is the field of hybrid electrochemical capacitors (HECs). Unlike EDLCs or pseudocapacitive ECs, HECs combine a faradic battery electrode with a capacitive or pseudocapacitive electrode. In these systems, the battery electrode brings the energy while the power comes from the capacitive one. Most of the popular HECs currently commercialized combine a Li-ion-battery graphite anode with a porous-carbon capacitive electrode. These are known as Li-ion capacitors (LIC)¹⁰¹, such as shown in Fig. 5a,b. The high operating cell voltage (3.8–2.2 V) of LICs comes from the use of the graphite anode and the SEI layer formation.

High energy density (beyond 20 Wh kg⁻¹) can be achieved using LIC technology, and the growing number of companies developing LICs demonstrate the interest in this technology, applications of which are similar to those of ECs. However, LICs are not expected to replace ECs, since they face several challenges¹⁰¹. The negative Li-ion graphite anode needs to be highly over-capacitive to accept high recharge rates (beyond the capacity of the limiting positive electrode), limiting the power capability to a few kilowatts per kilogram, which is a major difference from EDLCs. Also, the negative electrode must be prelithiated, which is achieved by introducing a sacrificial Li-metal electrode in the cell, short-circuited with the graphite anode before use. Although some smart solutions have been proposed that use sacrificial Li⁺ extraction at the positive electrode during the first cycle to balance the electrode capacities¹⁰², this limits to some extent the gravimetric and volumetric performance of the cells. Then, the use of carbonate-based electrolytes restrains the operating temperature range to that of Li-ion batteries, in contrast to EDLCs, which can use carbonate-free electrolytes¹⁰¹. Finally, the cycling life — and specially the impact of high charge/discharge rates on the negative electrode stability upon cycling — needs to be improved, despite hundreds of thousands of cycles being claimed by manufacturers¹⁰¹. However, thanks to the recent development of high-rate carbon-based materials for Li-ion-battery anodes³ and discovery or design of better pseudocapacitive materials⁷⁴, there is a chance of improving the LICs' energy density beyond 20 Wh kg⁻¹ using those nanostructured high-rate electrodes, while keeping high power capability close to that of EDLC (Fig. 5c,d). This would result in a major change in possible applications of ECs. In such designs, the presence of a Li-containing positive electrode, such as defective LFP, minimizes the need for an extra lithium source to form the SEI at the negative electrode. One concern might still be the cycling life of pseudocapacitive ECs compared with EDLCs, since the introduction of a redox-based charge-storage mechanism may result in chemical modification or volume change of the materials. This should be a target of future studies.

The HECs (Li-ion capacitors, for instance) that have recently appeared in the market currently offer the highest performance in terms of energy density (>20 Wh kg⁻¹). However, the use of a Li-ion-battery negative electrode in LIC systems limits their power capability compared with EDLCs and makes the cycle life during high-rate cycles uncertain. Also, HECs will face competition from high-power batteries such as the high-rate batteries, based on

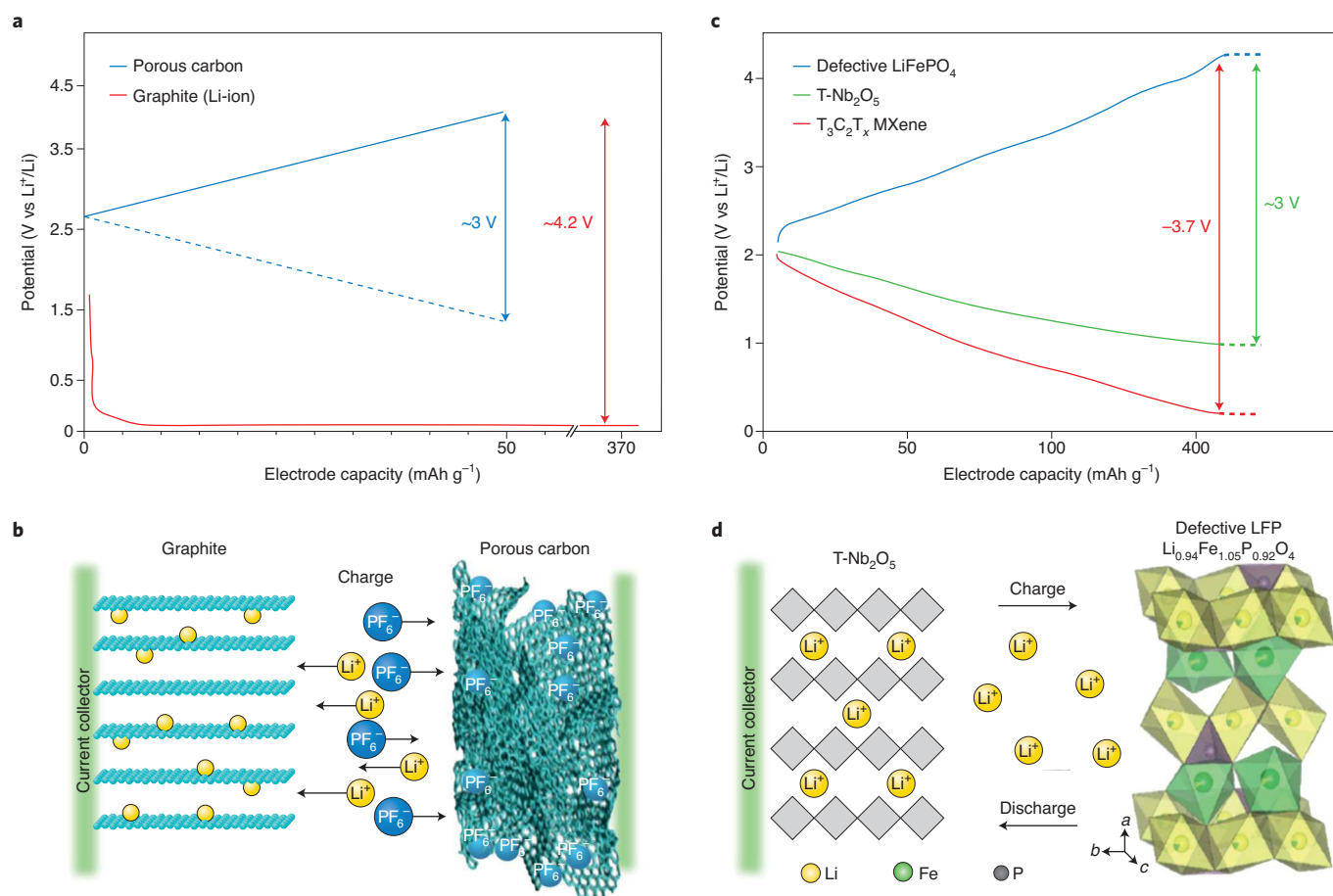


Fig. 5 | Lithium-ion capacitors. **a,b**, Concept of a Li-ion capacitor (LIC), which combines a negative graphite electrode, as used in a Li-ion battery, with a positive porous carbon EDLC electrode. The cell voltage is increased relative to an EDLC capacitor using symmetrical porous carbon electrodes. **c,d**, Concepts to show that high-power batteries and high-energy ECs using pseudocapacitive materials share similar features. Here, a combination of pseudocapacitive Nb₂O₅ or MXene negative electrode with a defective LFP positive electrode with sloping profile suggests the possibility of building a pseudocapacitive device.

lithium titanium oxide, developed by Toshiba¹⁰³, or emerging Na-ion batteries², which show similar power performance with a higher energy density.

Micro-devices for IoT and wearable electronics

The development of connected and smart environments, more commonly termed IoT¹⁰⁴, is a major emerging application for microscale energy-storage devices (Fig. 6a). IoT relies on the use of connected sensor networks that collect and transfer the data to a central gateway. It covers a broad range of applications: health (individual management and continuous monitoring of patients), environmental (fire prevention, air and water quality measurements) or industrial and infrastructure monitoring (buildings, bridges, roads and even museums), drug delivery (in vivo application), transportation, wearable personal electronics and various radiofrequency identification systems¹⁰⁴. Those applications require a very large number of compact, efficient, miniaturized energy-storage devices for energy delivery or harvesting with high power capabilities. Although micro-batteries can ensure a low continuous energy delivery, they fail to deliver the peak power needed for data acquisition and transfer. Moreover, their charge-storage capability per weight or volume of the device decreases with decreasing size, because of the increasing ratio of passive (packaging and so on) to active components.

Starting from about 2010, research on the development of micro-supercapacitors (MSCs) integrated on Si wafers, produced

on flexible substrates, printed on various surfaces or incorporated into textiles has been growing quickly to address these needs¹⁰⁵. Development of micro-devices is an emerging topic, but the field is quickly expanding, and there are high expectations in the design of high-energy and high-power micro-devices to support the development of the IoT¹⁰⁶.

MSCs can be prepared on various substrates using many techniques; the process chosen usually depends on the substrate¹⁰⁷. MSC devices are generally prepared in one of two designs, with stacked or planar interdigitated electrodes (Fig. 6b). In planar interdigitated electrodes, the areal capacitance per electrode polarity is 4 times the total areal capacitance of the device (footprint area)¹⁰⁷. Although MSCs share with their EC counterparts the challenge of high energy density, gravimetric performance has little meaning in this case. Reliable performance metrics are areal energy (Wh cm⁻²) and power (W cm⁻²) densities, or volumetric energy (Wh cm⁻³) and power (W cm⁻³) densities — calculated from areal (F cm⁻²) and volumetric (F cm⁻³) capacitance — to take into account the electrode thickness (Fig. 6c)¹⁰⁵. In addition to these metrics, the thickness of the substrate should be indicated as well as the electrode thickness or/and the total thickness of the device. A further challenge in MSCs is the preparation of mechanically stable electrodes with strong adhesion to the substrate and ability to withstand multiple deformation cycles, which are required in the case of flexible and wearable electronics.

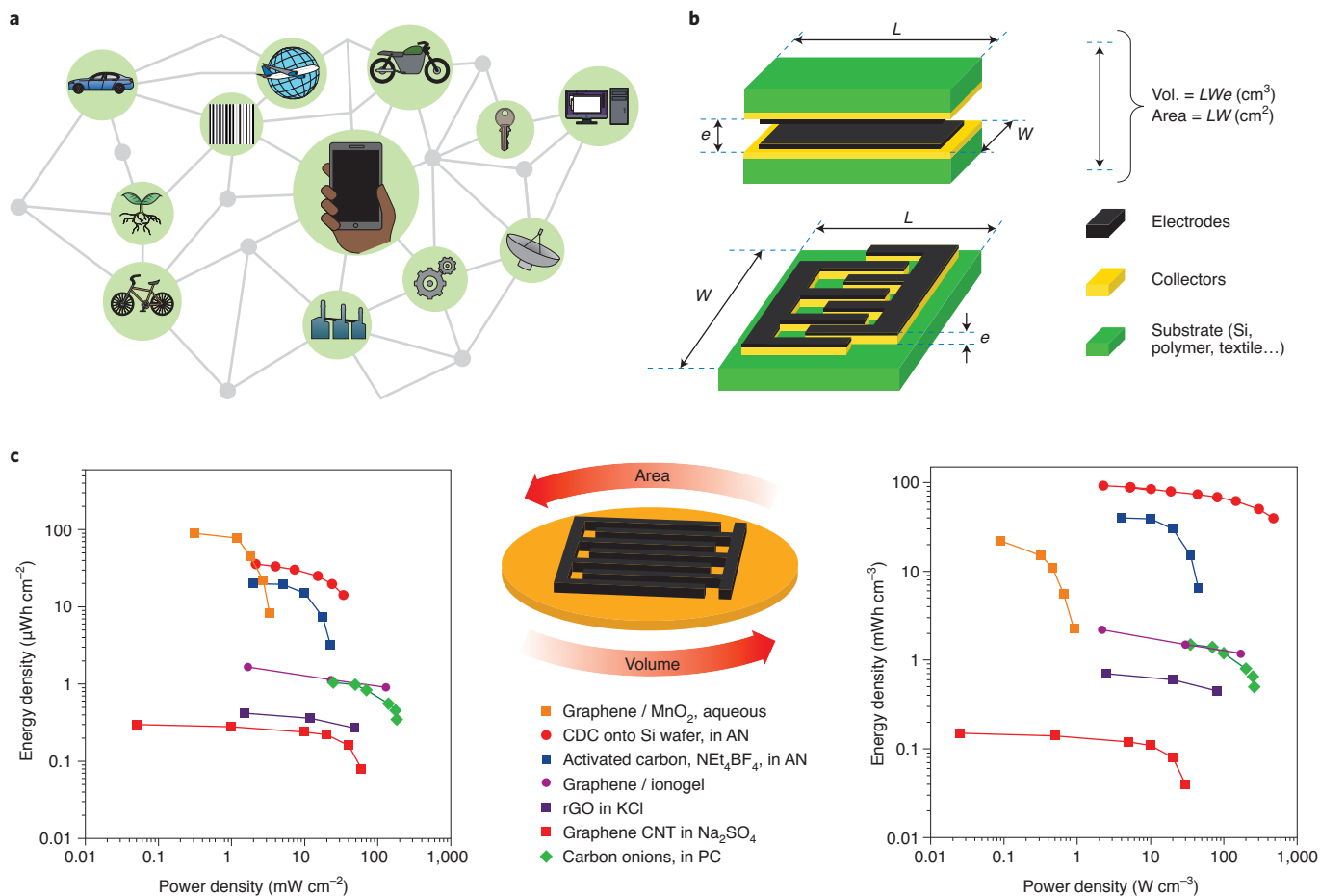


Fig. 6 | Micro-supercapacitors for current and future technologies. **a**, Sketch of a connected network of sensors used for the IoT. **b**, Calculations of areal and volumetric capacitance of micro-devices with planar (top) or interdigitated (bottom) electrode configuration. **c**, Example of Ragone plots showing the performance of MSC devices normalized per surface area (left) and volume (right). AN, acetonitrile; CNT, carbon nanotube; rGO, reduced graphene oxide. Adapted with permission from ref. ¹⁰⁶, AAAS.

The direct integration of MSCs on Si wafers is the most challenging concept, since fabrication techniques compatible with the semiconductor industry have to be used. Dry processing (atomic layer deposition or magnetron sputtering) is preferred to wet routes (such as electrophoretic or electrochemical deposition, screen printing or serigraphy), but the limited electrode thickness achieved by these techniques results in low areal capacitance¹⁰⁷. An important step forward was achieved by preparing on-chip MSCs by chlorination of TiC films ($\sim 5 \mu\text{m}$ thick) deposited on Si wafer by magnetron sputtering¹⁰⁶. The partial chlorination of TiC led to the formation of mechanically stable porous carbon electrodes strongly adhering to the Si surface. Electrode areal capacitance beyond 400 mF cm^{-2} was achieved in sulfuric acid electrolyte, making these micro-devices among the best reported for carbon-based MSCs (Fig. 6c). A limitation of the MSC technology based on nanoporous carbon electrodes is that it is barely compatible with the deposition of inorganic solid-state electrolytes owing to the electrode porosity, although solid-state-like electrolytes (gels or ionogels) can be used^{108,109}. Further improvement of the areal capacitance can be achieved by developing a 3D Si surface and preparing structures with high area enhancement factor (that is, the projected area per footprint area)¹⁰⁵. This offers interesting routes for preparing on-chip MSCs with a high areal energy density, using carbide-derived carbon electrodes prepared by the chlorination of TiC or other carbide films deposited by magnetron sputtering. Unfortunately, the vacuum

deposition of pseudocapacitive materials is more complex and limited to a few compounds, resulting in areal capacitance and energy density values below the expectations for practical applications¹⁰⁵. Electrochemical deposition techniques can also be used to prepare on-chip pseudocapacitive MSCs, with the same limitations in terms of the variety of materials and energy density.

A massive trend currently observed in the field of MSCs is the preparation of flexible devices aiming to address the need for smart textiles and for paper-based and flexible power electronics¹¹⁰. A major step has been the development of the laser-writing process technique, thanks to pioneering work from Kaner and co-workers, who reported the fabrication of MSCs by direct reduction of graphite oxide film under a laser beam in 2012, drawing porous 'laser-scribed graphene' interdigitated devices¹¹¹. Despite limited capacitance achieved (about 5 mF cm^{-2}) because of the thin electrodes, this was important in showing that a simple, easy to implement and scalable technique was efficient in preparation of flexible electrodes and micro-devices. Tour's group also showed the possibility of direct conversion of polymer substrates into carbon under the laser beam¹¹². Moving further, Kaner and co-workers functionalized laser-scribed graphene electrodes by electrochemical deposition of pseudocapacitive MnO_2 (ref. ¹¹³), resulting in a notable improvement in areal capacitance and energy density. The next challenges for this promising laser-scribing technology will be to implement newly developed pseudocapacitive materials, such as Nb_2O_5 , MoO_3

or MXene⁷⁴, operating in non-aqueous electrolytes to boost the energy performance. The technique will need to be adapted to those materials, since oxides require metal current collectors and MXenes may oxidize under the laser beam.

Besides laser writing, electrophoretic¹¹⁴, electrochemical¹¹⁵, stamping, spray coating and printing¹¹⁶ techniques have been used to prepare electrodes made of carbon and pseudocapacitive materials on flexible substrates. Conventional and 3D printing on a variety of surfaces are experiencing fast expansion¹¹⁶. The areal capacitance achieved ranges from $<1 \text{ mF cm}^{-2}$ to hundreds of mF cm^{-2} , depending on the material used and the electrode thickness¹¹⁶. Although the field is still young, some trends can be extracted from the literature survey. First, the mechanical properties and the quality of the electrode/current-collector interface (adherence of the film) have a strong impact on the performance and the cycle life of the devices. Thus, deposition techniques leading to improved impedance of the contact — electrochemical plating, for instance — are preferred. The preparation of carbon nanotube, graphene or reduced graphene oxide electrodes leads to a moderate areal capacitance (less than about 20 mF cm^{-2}) owing to limited electrode thickness; electrodeposition of pseudocapacitive materials (such as MnO_2 , RuO_2 or conducting polymers) in an additional synthesis step allows for great improvement of the areal capacitance to $200\text{--}300 \text{ mF cm}^{-2}$. However, the use of aqueous electrolytes comes with a narrow cell voltage (less than $\sim 1.6 \text{ V}$) and energy density limitation, as discussed earlier. The situation is different for carbon-based MSCs which can operate in non-aqueous electrolytes, with the highest capacitance being reported so far for porous carbons with a high surface area. The use of highly conductive graphene and MXene eliminates the need for metal current collectors, greatly simplifying the manufacturing process. Finally, the use of increasingly popular solid-state-like (gel) electrolytes may resolve the issue of electrolyte leakage and eliminate the need for hermetically sealed packaging¹¹⁶.

However, MSCs will have to address several challenges in the near future to meet industry expectations. Solid-state or gel high-voltage electrolytes are needed to replace the aqueous polyvinyl-alcohol-based gel electrolytes with a narrow voltage window (about 1 V in acids). Developing inorganic ceramic solid-state electrolyte will be challenging owing to the high surface area of carbon materials and the general issues of mastering the electrolyte/active material interfaces. Alternatively, ionogel electrolytes (that is, ionic liquid phase entrapped inside an inorganic (SiO_2) matrix) have been successfully used in ECs in combination with high-surface-area materials, offering voltage windows up to 3 V (refs. ^{108,109}). Also, transferring the recent advances in the pseudocapacitive field, such as the use of bulk intercalation pseudocapacitance mechanism (Nb_2O_5 , MoO_3 or MXene), operating in non-aqueous electrolyte into real micro-devices would result in a major enhancement of both the areal capacitance and the energy density^{86,90,97}. The design of a suitable 3D electrode structure would further boost the areal power and energy performance^{113,115}. Finally, the combination of the pseudocapacitive materials with suitable electrodes using 1D, 2D and/or 3D carbon structures or even high-rate battery materials would result in major improvements, making MSC devices competitive with micro-batteries for applications in embedded sensors for battery monitoring, truly wearable systems integrated into clothes, or energy harvesting.

As a separate class of emerging flexible devices, we need to consider textile supercapacitors. This area emerged less than ten years ago¹¹⁷ and keeps growing because of the interest in ‘wearable Internet’ and smart textiles¹¹⁰. Initially, carbon materials were used, but conductive polymers, metal oxides¹¹⁸ and MXenes¹¹⁹ recently entered the field. Storing the amount of energy required for powering devices, from LEDs to sensors and communication (antennas) on the limited surface of a garment (less than 1 m^2) is challenging, if only EDLC is used. Energy-storing textiles have some additional requirements to materials, such as stretchability, washability and

biosafety, when in direct contact with skin. This puts certain restrictions on choice of active materials and electrolytes, which should be gels or polymers. Also, the capacitance and other characteristics should be normalized by length of fibres and yarns (F cm^{-1}) or area for textiles (F cm^{-2}), as gravimetric data for the active material itself do not really help to understand how much charge can be stored in the garment¹¹⁷. This is a quickly maturing research area, and rapid development is expected in the next few years.

Summary and outlook

This Review aims at providing general key messages. The first is that EDLCs have certain features (no redox processes, long cycle life, high power and a wide temperature range of operation) that make them an important technology for energy-storage applications. The energy density of EDLCs can be increased by increasing the cell voltage via interface modification or development of chemically stable, high-surface-area carbon structures free from defects and functional groups.

Next, the recent discoveries of new pseudocapacitive materials and of the bulk intercalation pseudocapacitive reaction mechanism occurring in non-aqueous electrolytes are examples of key advances in the field of capacitive storage, since high-energy and high-power electrodes and devices can now be produced. Here, the high-power challenge for batteries meets the high-energy quest for ECs, and the combination can make a huge impact on the entire energy-storage field.

The IoT is currently pushing the development of MSC technology, and several techniques and processes have been developed to prepare MSCs with a focus on flexible devices. The laser-based techniques, ink-jet printing, stamping, 3D printing and other processes used are very different from conventional tape electrode manufacturing. To meet the needs of flexible and wearable technology, new materials and new device designs should be implemented. Active materials with very high electronic conductivity are required to eliminate current collectors. The use of conductive 1D and 2D materials could eliminate the need for resistive polymer binders. Non-leaking gel and polymer electrolytes are needed to eliminate special packaging and enable textile supercapacitors. A coating technology should be developed for separation of electrodes (gel and polymer electrolytes can play the role of separators) and encapsulation of devices (for example, polymer spray-coating or vapour deposition). Conventional sandwich device designs will be replaced by interdigitated electrodes and fibres/yarns.

Received: 27 December 2019; Accepted: 18 June 2020;

Published online: 03 August 2020

References

1. Simon, P. & Gogotsi, Y. Materials for electrochemical capacitors. *Nat. Mater.* **7**, 845–854 (2008).
2. Delmas, C. Sodium and sodium-ion batteries: 50 years of research. *Adv. Energy Mater.* **8**, 1703137 (2018).
3. Li, M., Lu, J., Chen, Z. & Amine, K. 30 years of lithium-ion batteries. *Adv. Mater.* **30**, 1800561 (2018).
4. Palacin, M. R. & de Guibert, A. Why do batteries fail? *Science* **351**, 1253292 (2016).
5. Augustyn, V., Simon, P. & Dunn, B. Pseudocapacitive oxide materials for high-rate electrochemical energy storage. *Energy Environ. Sci.* **7**, 1597–1614 (2014).
6. Liu, C. F., Liu, Y. C., Yi, T. Y. & Hu, C. C. Carbon materials for high-voltage supercapacitors. *Carbon* **145**, 529–548 (2019).
7. Wang, F. X. et al. Latest advances in supercapacitors: from new electrode materials to novel device designs. *Chem. Soc. Rev.* **46**, 6816–6854 (2017).
8. Wang, Y. G., Song, Y. F. & Xia, Y. Y. Electrochemical capacitors: mechanism, materials, systems, characterization and applications. *Chem. Soc. Rev.* **45**, 5925–5950 (2016).
9. Wu, H. et al. Graphene based architectures for electrochemical capacitors. *Energy Storage Mater.* **5**, 8–32 (2016).
10. Lin, Z. et al. Materials for supercapacitors: when Li-ion battery power is not enough. *Mater. Today* **21**, 419–436 (2018).

11. Noori, A., El-Kady, M. F., Rahmanifar, M. S., Kaner, R. B. & Mousavi, M. F. Towards establishing standard performance metrics for batteries, supercapacitors and beyond. *Chem. Soc. Rev.* **48**, 1272–1341 (2019).
12. Salanne, M. et al. Efficient storage mechanisms for building better supercapacitors. *Nat. Energy* **1**, 16070 (2016).
13. Miller, J. R., Outlaw, R. A. & Holloway, B. C. Graphene double-layer capacitor with ac line-filtering performance. *Science* **329**, 1637–1639 (2010).
14. Horn, M., MacLeod, J., Liu, M., Webb, J. & Motta, N. Supercapacitors: a new source of power for electric cars? *Econ. Anal. Policy* **61**, 93–103 (2019).
15. Ultracapacitor modules. *Maxwell Technologies* <https://www.maxwell.com/products/ultracapacitors/modules> (accessed May 2020).
16. *LS Ultracapacitor* <https://www.ultracapacitor.co.kr:8001/> (accessed May 2020).
17. *Skeleton Technologies* <https://www.skeletontech.com/> (accessed May 2020).
18. Gogotsi, Y. & Simon, P. True performance metrics in electrochemical energy storage. *Science* **334**, 917–918 (2011).
19. Mathis, T. S. et al. Energy storage data reporting in perspective — guidelines for interpreting the performance of electrochemical energy storage systems. *Adv. Energy Mater.* **9**, 1902007 (2019).
20. Conway, B. *Electrochemical Supercapacitors; Scientific Fundamentals and Technological Applications* (Springer, 1999).
21. Shao, H., Wu, Y.-C., Lin, Z., Taberna, P.-L. & Simon, P. Nanoporous carbon for electrochemical capacitive energy storage. *Chem. Soc. Rev.* **49**, 3005–3039 (2020).
22. Lin, T. Q. et al. Nitrogen-doped mesoporous carbon of extraordinary capacitance for electrochemical energy storage. *Science* **350**, 1508–1513 (2015).
23. Beguin, F., Presser, V., Balducci, A. & Frackowiak, E. Carbons and electrolytes for advanced supercapacitors. *Adv. Mater.* **26**, 2219–2251 (2014).
24. Zhong, C. et al. A review of electrolyte materials and compositions for electrochemical supercapacitors. *Chem. Soc. Rev.* **44**, 7484–7539 (2015).
25. Miller, J. R. & Butler, S. M. Electrical characteristics of large state-of-the-art electrochemical capacitors. *Electrochim. Acta* **307**, 564–572 (2019).
26. Xiong, G., Kundu, A. & Fisher, S. T. *Thermal Effects in Supercapacitors* (Springer, 2015).
27. Prehal, C. et al. Quantification of ion confinement and desolvation in nanoporous carbon supercapacitors with modelling and in situ X-ray scattering. *Nat. Energy* **2**, 16215 (2017).
28. Forse, A. C. et al. Direct observation of ion dynamics in supercapacitor electrodes using in situ diffusion NMR spectroscopy. *Nat. Energy* **2**, 16216 (2017).
29. Chmiola, J. et al. Anomalous increase in carbon capacitance at pore sizes less than 1 nanometer. *Science* **313**, 1760–1763 (2006).
30. Forse, A. C., Merlet, C., Griffin, J. M. & Grey, C. P. New perspectives on the charging mechanisms of supercapacitors. *J. Am. Chem. Soc.* **138**, 5731–5744 (2016).
31. Griffin, J. M. et al. In situ NMR and electrochemical quartz crystal microbalance techniques reveal the structure of the electrical double layer in supercapacitors. *Nat. Mater.* **14**, 812–819 (2015).
32. Deschamps, M. et al. Exploring electrolyte organization in supercapacitor electrodes with solid-state NMR. *Nat. Mater.* **12**, 351–358 (2013).
33. Boukhalfa, S. et al. In situ small angle neutron scattering revealing ion sorption in microporous carbon electrical double layer capacitors. *ACS Nano* **8**, 2495–2503 (2014).
34. Batisse, N. & Raymundo-Pinero, E. Pulsed electrochemical mass spectrometry for operando tracking of interfacial processes in small-time-constant electrochemical devices such as supercapacitors. *ACS Appl. Mater. Interfaces* **9**, 41224–41232 (2017).
35. Kim, J. et al. Nondisruptive in situ Raman analysis for gas evolution in commercial supercapacitor cells. *Electrochim. Acta* **219**, 447–452 (2016).
36. Richey, F. W., Dyatkin, B., Gogotsi, Y. & Elabd, Y. A. Ion dynamics in porous carbon electrodes in supercapacitors using in situ infrared spectroelectrochemistry. *J. Am. Chem. Soc.* **135**, 12818–12826 (2013).
37. Kondrat, S., Wu, P., Qiao, R. & Kornyshev, A. A. Accelerating charging dynamics in subnanometre pores. *Nat. Mater.* **13**, 387–393 (2014).
38. Pean, C. et al. On the dynamics of charging in nanoporous carbon-based supercapacitors. *ACS Nano* **8**, 1576–1583 (2014).
39. Merlet, C. et al. On the molecular origin of supercapacitance in nanoporous carbon electrodes. *Nat. Mater.* **11**, 306–310 (2012).
40. Kondrat, S. & Kornyshev, A. Superionic state in double-layer capacitors with nanoporous electrodes. *J. Phys. Condens. Matter* **23**, 022201 (2011).
41. Bi, S. et al. Molecular understanding of charge storage and charging dynamics in supercapacitors with MOF electrodes and ionic liquid electrolytes. *Nat. Mater.* **19**, 552–558 (2020).
42. Tsai, W. Y., Taberna, P. L. & Simon, P. Electrochemical quartz crystal microbalance (EQCM) study of ion dynamics in nanoporous carbons. *J. Am. Chem. Soc.* **136**, 8722–8728 (2014).
43. Shpigel, N., Levi, M. D., Sigalov, S., Daikhin, L. & Aurbach, D. In situ real-time mechanical and morphological characterization of electrodes for electrochemical energy storage and conversion by electrochemical quartz crystal microbalance with dissipation monitoring. *Acc. Chem. Res.* **51**, 69–79 (2018).
44. Shpigel, N. et al. In situ hydrodynamic spectroscopy for structure characterization of porous energy storage electrodes. *Nat. Mater.* **15**, 570–575 (2016).
45. Le, T. et al. Unveiling the ionic exchange mechanisms in vertically-oriented graphene nanosheet supercapacitor electrodes with electrochemical quartz crystal microbalance and ac-electrogravimetry. *Electrochem. Commun.* **93**, 5–9 (2018).
46. Umeda, K., Kobayashi, K., Minato, T. & Yamada, H. Atomic-scale three-dimensional local solvation structures of ionic liquids. *J. Phys. Chem. Lett.* **11**, 1343–1348 (2020).
47. Tsai, W.-Y. et al. Hysteretic order–disorder transitions of ionic liquid double layer structure on graphite. *Nano Energy* **60**, 886–893 (2019).
48. Ye, J. L. et al. Charge storage mechanisms of single-layer graphene in ionic liquid. *J. Am. Chem. Soc.* **141**, 16559–16563 (2019).
49. Mao, X. et al. Self-assembled nanostructures in ionic liquids facilitate charge storage at electrified interfaces. *Nat. Mater.* **18**, 1350–1357 (2019).
50. Jackel, N., Simon, P., Gogotsi, Y. & Presser, V. Increase in capacitance by subnanometer pores in carbon. *ACS Energy Lett.* **1**, 1262–1265 (2016).
51. Yan, R. Y., Antonietti, M. & Oschatz, M. Toward the experimental understanding of the energy storage mechanism and ion dynamics in ionic liquid based supercapacitors. *Adv. Energy Mater.* **8**, 1800026 (2018).
52. Antonietti, M., Chen, X. D., Yan, R. Y. & Oschatz, M. Storing electricity as chemical energy: beyond traditional electrochemistry and double-layer compression. *Energy Environ. Sci.* **11**, 3069–3074 (2018).
53. Futamura, R. et al. Partial breaking of the Coulombic ordering of ionic liquids confined in carbon nanopores. *Nat. Mater.* **16**, 1225–1232 (2017).
54. Bazant, M. Z., Storey, B. D. & Kornyshev, A. A. Double layer in ionic liquids: overscreening versus crowding. *Phys. Rev. Lett.* **106**, 046102 (2011).
55. Liu, Y. M., Merlet, C. & Smit, B. Carbons with regular pore geometry yield fundamental insights into supercapacitor charge storage. *ACS Cent. Sci.* **5**, 1813–1823 (2019).
56. Redondo, E. et al. Outstanding room-temperature capacitance of biomass-derived microporous carbons in ionic liquid electrolyte. *Electrochem. Commun.* **79**, 5–8 (2017).
57. Miller, J. R. & Burke, A. F. Electrochemical capacitors: challenges and opportunities for real-world applications. *Electrochem. Soc. Interface* **8**, 53–57 (2008).
58. Pognon, G., Brousse, T., Demarconnay, L. & Belanger, D. Performance and stability of electrochemical capacitor based on anthraquinone modified activated carbon. *J. Power Sources* **196**, 4117–4122 (2011).
59. Assreshegn, B. D., Brousse, T. & Belanger, D. Advances on the use of diazonium chemistry for functionalization of materials used in energy storage systems. *Carbon* **92**, 362–381 (2015).
60. Nomura, K., Nishihara, H., Kobayashi, N., Asada, T. & Kyotani, T. 4.4 V supercapacitors based on super-stable mesoporous carbon sheet made of edge-free graphene walls. *Energy Environ. Sci.* **12**, 1542–1549 (2019).
61. Antonietti, M. & Oschatz, M. The concept of ‘noble, heteroatom-doped carbons’, their directed synthesis by electronic band control of carbonization, and applications in catalysis and energy materials. *Adv. Mater.* **30**, 1706836 (2018).
62. Schutter, C., Passerini, S., Korth, M. & Balducci, A. Cyano ester as solvent for high voltage electrochemical double layer capacitors. *Electrochim. Acta* **224**, 278–284 (2017).
63. Krummacher, J., Schütter, C., Hess, L. H. & Balducci, A. Non-aqueous electrolytes for electrochemical capacitors. *Curr. Opin. Electrochem.* **9**, 64–69 (2018).
64. Xie, H. J., Gelin, B. & Rochefort, D. Redox-active electrolyte supercapacitors using electroactive ionic liquids. *Electrochem. Commun.* **66**, 42–45 (2016).
65. Mourad, E. et al. Biredox ionic liquids with solid-like redox density in the liquid state for high-energy supercapacitors. *Nat. Mater.* **16**, 446–453 (2017).
66. Birkel, C. R., Roberts, M. R., McTurk, E., Bruce, P. G. & Howey, D. A. Degradation diagnostics for lithium ion cells. *J. Power Sources* **341**, 373–386 (2017).
67. Singh, N. et al. Artificial SEI transplantation: a pathway to enabling lithium metal cycling in water-containing electrolyte. *ACS Appl. Energy Mater.* **2**, 8912–8918 (2019).
68. Son, S. B. et al. An artificial interphase enables reversible magnesium chemistry in carbonate electrolytes. *Nat. Chem.* **10**, 532–539 (2018).
69. Brandon, E. J., West, W. C., Smart, M. C., Whitcanack, L. D. & Plett, G. A. Extending the low temperature operational limit of double-layer capacitors. *J. Power Sources* **170**, 225–232 (2007).
70. Kunze, M. et al. Mixtures of ionic liquids for low temperature electrolytes. *Electrochim. Acta* **82**, 69–74 (2012).
71. Tsai, W. Y. et al. Outstanding performance of activated graphene based supercapacitors in ionic liquid electrolyte from –50 to 80 °C. *Nano Energy* **2**, 403–411 (2013).

72. Premathilake, D. et al. Fast response, carbon-black-coated, vertically-oriented graphene electric double layer capacitors. *J. Electrochem. Soc.* **165**, A924–A931 (2018).
73. Miller, J. R. & Outlaw, R. A. Vertically-oriented graphene electric double layer capacitor designs. *J. Electrochem. Soc.* **162**, A5077–A5082 (2015).
74. Choi, C. et al. Achieving high energy density and high power density with pseudocapacitive materials. *Nat. Rev. Mater.* **5**, 5–19 (2020).
75. Lee, H. Y. & Goodenough, J. B. Supercapacitor behavior with KCl electrolyte. *J. Solid State Chem.* **144**, 220–223 (1999).
76. Brousse, T., Belanger, D. & Long, J. W. To be or not to be pseudocapacitive? *J. Electrochem. Soc.* **162**, A5185–A5189 (2015).
77. Simon, P., Gogotsi, Y. & Dunn, B. Where do batteries end and supercapacitors begin? *Science* **343**, 1210–1211 (2014).
78. Lukatskaya, M. R., Dunn, B. & Gogotsi, Y. Multidimensional materials and device architectures for future hybrid energy storage. *Nat. Commun.* **7**, 12647 (2016).
79. Wang, J., Polleux, J., Lim, J. & Dunn, B. Pseudocapacitive contributions to electrochemical energy storage in TiO₂ (anatase) nanoparticles. *J. Phys. Chem. C* **111**, 14925–14931 (2007).
80. Ko, J. S., Sassin, M. B., Rolison, D. R. & Long, J. W. Deconvolving double-layer, pseudocapacitance, and battery-like charge-storage mechanisms in nanoscale LiMn₂O₄ at 3D carbon architectures. *Electrochim. Acta* **275**, 225–235 (2018).
81. Gibson, A. J. & Donne, S. W. A step potential electrochemical spectroscopy (SPECS) investigation of anodically electrodeposited thin films of manganese dioxide. *J. Power Sources* **359**, 520–528 (2017).
82. Shao, H., Lin, Z., Xu, K., Taberna, P.-L. & Simon, P. Electrochemical study of pseudocapacitive behavior of Ti₃C₂T_x MXene material in aqueous electrolytes. *Energy Storage Mater.* **18**, 456–461 (2019).
83. Costentin, C. & Saveant, J. M. Energy storage: pseudocapacitance in prospect. *Chem. Sci.* **10**, 5656–5666 (2019).
84. Naguib, M. et al. Two-dimensional nanocrystals produced by exfoliation of Ti₃AlC₂. *Adv. Mater.* **23**, 4248–4253 (2011).
85. Anasori, B., Lukatskaya, M. R. & Gogotsi, Y. 2D metal carbides and nitrides (MXenes) for energy storage. *Nat. Rev. Mater.* **2**, 16098 (2017).
86. Wang, X. et al. Influences from solvents on charge storage in titanium carbide MXenes. *Nat. Energy* **4**, 241–248 (2019).
87. Lukatskaya, M. R. et al. Cation intercalation and high volumetric capacitance of two-dimensional titanium carbide. *Science* **341**, 1502–1505 (2013).
88. Lukatskaya, M. R. et al. Ultra-high-rate pseudocapacitive energy storage in two-dimensional transition metal carbides. *Nat. Energy* **2**, 17105 (2017).
89. Ghidui, M., Lukatskaya, M. R., Zhao, M. Q., Gogotsi, Y. & Barsoum, M. W. Conductive two-dimensional titanium carbide ‘clay’ with high volumetric capacitance. *Nature* **516**, 78–81 (2014).
90. Augustyn, V. et al. High-rate electrochemical energy storage through Li⁺ intercalation pseudocapacitance. *Nat. Mater.* **12**, 518–522 (2013).
91. Girard, H. L., Dunn, B. & Pilon, L. Simulations and interpretation of three-electrode cyclic voltammograms of pseudocapacitive electrodes. *Electrochim. Acta* **211**, 420–429 (2016).
92. Conway, B. E. Two-dimensional and quasi two-dimensional isotherms for Li intercalation and UPD processes at surfaces. *Electrochim. Acta* **38**, 1249–1258 (1993).
93. Li, Y. et al. A general Lewis acidic etching route for preparing MXenes with enhanced electrochemical performance in non-aqueous electrolyte. *Nat. Mater.* **19**, 894–899 (2020).
94. Naoi, K. et al. Ultrafast charge–discharge characteristics of a nanosized core–shell structured LiFePO₄ material for hybrid supercapacitor applications. *Energy Environ. Sci.* **9**, 2143–2151 (2016).
95. Amisse, R. et al. Singular structural and electrochemical properties in highly defective LiFePO₄ powders. *Chem. Mater.* **27**, 4261–4273 (2015).
96. Okubo, M. et al. Nanosize effect on high-rate Li-ion intercalation in LiCoO₂ electrode. *J. Am. Chem. Soc.* **129**, 7444–7452 (2007).
97. Kim, H. S. et al. Oxygen vacancies enhance pseudocapacitive charge storage properties of MoO_{3-x}. *Nat. Mater.* **16**, 454–460 (2017).
98. Wang, R. C. et al. Operando atomic force microscopy reveals mechanics of structural water driven battery-to-pseudocapacitor transition. *ACS Nano* **12**, 6032–6039 (2018).
99. Mitchell, J. B. et al. Confined interlayer water promotes structural stability for high-rate electrochemical proton intercalation in tungsten oxide hydrates. *ACS Energy Lett.* **4**, 2805–2812 (2019).
100. Yamada, Y., Wang, J., Ko, S., Watanabe, E. & Yamada, A. Advances and issues in developing salt-concentrated battery electrolytes. *Nat. Energy* **4**, 269–280 (2019).
101. Han, P. X. et al. Lithium ion capacitors in organic electrolyte system: scientific problems, material development, and key technologies. *Adv. Energy Mater.* **8**, 1801243 (2018).
102. Jezowski, P. et al. Safe and recyclable lithium-ion capacitors using sacrificial organic lithium salt. *Nat. Mater.* **17**, 167–173 (2018).
103. Takami, N. et al. High-energy, fast-charging, long-life lithium-ion batteries using TiNb₂O₇ anodes for automotive applications. *J. Power Sources* **396**, 429–436 (2018).
104. Whitmore, A., Agarwal, A. & Xu, L. D. The Internet of Things — a survey of topics and trends. *Inform. Syst. Front.* **17**, 261–274 (2015).
105. Lethien, C., Le Bideau, J. & Brousse, T. Challenges and prospects of 3D micro-supercapacitors for powering the internet of things. *Energy Environ. Sci.* **12**, 96–115 (2019).
106. Huang, P. et al. On-chip and freestanding elastic carbon films for micro-supercapacitors. *Science* **351**, 691–695 (2016).
107. Kyeremateng, N. A., Brousse, T. & Pech, D. Microsupercapacitors as miniaturized energy-storage components for on-chip electronics. *Nat. Nanotechnol.* **12**, 7–15 (2017).
108. Negre, L., Daffos, B., Turq, V., Taberna, P. L. & Simon, P. Ionogel-based solid-state supercapacitor operating over a wide range of temperature. *Electrochim. Acta* **206**, 490–495 (2016).
109. Brachet, M., Brousse, T. & Le Bideau, J. All solid-state symmetrical activated carbon electrochemical double layer capacitors designed with ionogel electrolyte. *ECS Electrochem. Lett.* **3**, A112–A115 (2014).
110. Sumboja, A. et al. Electrochemical energy storage devices for wearable technology: a rationale for materials selection and cell design. *Chem. Soc. Rev.* **47**, 5919–5945 (2018).
111. El-Kady, M. F., Strong, V., Dubin, S. & Kaner, R. B. Laser scribing of high-performance and flexible graphene-based electrochemical capacitors. *Science* **335**, 1326–1330 (2012).
112. Lin, J. et al. Laser-induced porous graphene films from commercial polymers. *Nat. Commun.* **5**, 5714 (2014).
113. El-Kady, M. F. et al. Engineering three-dimensional hybrid supercapacitors and microsupercapacitors for high-performance integrated energy storage. *Proc. Natl Acad. Sci. USA* **112**, 4233–4238 (2015).
114. Ye, L. H. et al. Highly efficient materials assembly via electrophoretic deposition for electrochemical energy conversion and storage devices. *Adv. Energy Mater.* **6**, 1502018 (2016).
115. Ferris, A., Garbarino, S., Guay, D. & Pech, D. 3D RuO₂ microsupercapacitors with remarkable areal energy. *Adv. Mater.* **27**, 6625–6629 (2015).
116. Zhang, Y. Z. et al. Printed supercapacitors: materials, printing and applications. *Chem. Soc. Rev.* **48**, 3229–3264 (2019).
117. Jost, K., Dion, G. & Gogotsi, Y. Textile energy storage in perspective. *J. Mater. Chem. A* **2**, 10776–10787 (2014).
118. Garcia-Torres, J., Roberts, A. J., Slade, R. C. T. & Crean, C. One-step wet-spinning process of CB/CNT/MnO₂ nanotubes hybrid flexible fibres as electrodes for wearable supercapacitors. *Electrochim. Acta* **296**, 481–490 (2019).
119. Quain, E. et al. Direct writing of additive-free MXene-in-water ink for electronics and energy storage. *Adv. Mater. Technol.* **4**, 1800256 (2019).

Acknowledgements

P.S. acknowledges H. Shao, P. Rozier and C. Merlet for help with the figures, as well as the Agence Nationale de la Recherche (Labex Store-Ex) and Institut Universitaire de France for support. Y.G.’s research on capacitive energy storage was primarily supported through the Fluid Interface Reactions, Structures, and Transport (FIRST) Center, an Energy Frontier Research Center funded by the US Department of Energy, Office of Science, and Office of Basic Energy Sciences.

Author contributions

Both authors contributed equally to the planning and writing of this article.

Competing interests

The authors declare no competing interests.

Additional information

Correspondence should be addressed to P.S. or Y.G.